# Impact of Loss Variations on Double-Ended Distributed Temperature Sensors Based on Raman Anti-Stokes Signal Only

Marcelo A. Soto, Alessandro Signorini, Tiziano Nannipieri, Stefano Faralli, Gabriele Bolognini, *Member, IEEE*, and Fabrizio Di Pasquale, *Member, IEEE*

*(Invited Paper)*

***Abstract*—We present a theoretical and experimental analysis of the sensing capabilities of Raman-based distributed temperature optical fiber sensor (RDTS) systems using only the anti-Stokes (AS) component in loop configuration. In particular, the effects of time- and wavelength-dependent losses on the sensor performance are thoroughly investigated under different experimental conditions. As expected from the developed theory, experimental results demonstrate that using the loop AS-light only approach in RDTS systems can correct the impact of local and wavelength-dependent losses on the final temperature measurements, with the simple use of an internal calibration fiber spool at a known temperature value. Signal-to-noise ratio and temperature resolution analyses of the AS-only RDTS point out an improved temperature resolution in comparison to standard RDTS systems in loop configuration.**

***Index Terms*—Distributed optical fiber sensors, optical time domain reflectometry, Raman scattering, temperature sensors.**

## I. Introduction

RAMAN-BASED DISTRIBUTED TEMPERATURE SENSORS (RDTSs) have been studied for many years [1]–[3] and, owing to the well-known advantages over their electrical counterparts, they have found successful applications in many different areas, such as fire detection, power cable monitoring and leakage detection. The vast majority of RDTS systems are based on optical time-domain-reflectometry (OTDR) measurements of the backscattered Raman anti-Stokes (AS) signal and either the Raman Stokes (S) or Rayleigh component [3]–[5]. Although single-ended RDTSs (where the fiber is interrogated from one fiber end only) represent the most common solution in long range applications due to their extended sensing distance [5], they are intrinsically affected by issues arising from the different fiber losses at the AS and S wavelengths and their time-dependent variations (such effects are commonly referred to wavelength-dependent losses, WDL, or differential attenuation, DA) [6]; their slow variation with time actually causes a slow and undetectable distortion in the measured temperature traces. This normally happens due to fiber-ageing (with a timescale of many years), but can be strongly enhanced in specific harsh application environments, such as in nuclear plants monitoring, where the presence of ionizing radiation effectively increases the optical fiber attenuation with time and induces significant WDL [6], [7]. It has also been shown that the fiber losses can be strongly enhanced by fiber degradation in hot and humid environments. Moreover, in geothermal wells applications, the differential wavelength-dependent attenuation of the fiber typically varies with time as a consequence of high temperature and Hydrogen concentration [8]. In practical RDTS systems, both WDL and local losses must be effectively taken into account and cancelled out; this can be done for instance by employing an alternate double-ended interrogation scheme (also called loop configuration technique) [6], where AS and S traces are subsequently acquired in forward and backward directions and then properly averaged [6]. For single-ended configurations, the use of AS-light only has been proposed in [9], together with a suitable reflective mirror at the far fiber-end. However, the four-fold optical path undergone by the light pulse and its scattering makes this technique not suitable for long-range sensing due to the high experienced losses. Moreover, the use of a strongly reflective mirror would make the system sensitive to multiple optical reflections (ghosts) with unknown connector conditions.

In this paper we perform a thorough theoretical and experimental study that confirms preliminary results on long-range RDTS systems based on a loop-scheme using AS-light only, employing a simple, single-channel receiver [10], [11]; experimental results now fully demonstrate the inherent correction of WDL and local losses of this method, being in good agreement with the developed theory and confirming the temperature resolution enhancement.

## II. Theory

### A. Generalities on Raman-Based Distributed Optical Fiber Sensors (RDTS)

Spontaneous Raman scattering (SpRS) is a temperature-dependent process caused by thermally driven molecular

Manuscript received June 30, 2011; revised September 15, 2011, October 19, 2011; accepted October 21, 2011. Date of publication November 07, 2011; date of current version March 21, 2012.

M. A. Soto, A. Signorini, T. Nannipieri, S. Faralli, and F. Di Pasquale are with TeCIP Institute, Scuola Superiore Sant'Anna, 56124 Pisa, Italy.

G. Bolognini is with IMM Institute, Consiglio Nazionale delle Ricerche, 40129 Bologna, Italy. He was with TeCIP Institute, Scuola Superiore Sant'Anna, 56124 Pisa, Italy (e-mail: bolognini@bo.imm.cnr.it).

Color versions of one or more of the figures in this paper are available online at http://ieeexplore.ieee.org.

Digital Object Identifier 10.1109/JLT.2011.2174966

vibrations, in which two spectral components shifted from the incoming light are generated [12]. In particular, the intensity of the Raman upshifted frequency component (anti-Stokes light) exhibits a strong dependence on the temperature, while the downshifted frequency component (Stokes light) is only slightly temperature dependent [5]. The temperature sensitivity of the spontaneous anti-Stokes Raman scattering is actually a well-known parameter, exhibiting a quasi-linear relative sensitivity of 0.8%/K at around room temperature, a value that slightly changes to 1.2%/K at around $-52°$C [2]. Although the absolute power of the AS Raman component is more than 30 dB weaker than the Rayleigh backscatterd component, its temperature dependence is high enough to provide a mechanism to perform distributed temperature sensing for real applications using an optical fiber [1]–[3].

In order to obtain the spatial information in RDTS systems, OTDR techniques are usually exploited [4]. This method is often called Raman-OTDR, and consists in launching short laser pulses into the sensing fiber and detecting the backscattered spontaneous Raman signal with high temporal resolution [2], [3].

Unfortunately, the AS Raman signal reaching the receiver does not only depend on the fiber temperature, but also on the fiber attenuation and local losses (such as splices, connectors and bending losses) [3]. This dependence can actually induce errors in the temperature measurements, since variations of the local fiber losses and attenuation coefficient at the AS wavelength can be easily misinterpreted as temperature variations. To overcome this problem, the AS Raman-OTDR trace has to be normalized by a temperature-independent OTDR signal, such as the Raman Stokes [3] or Rayleigh [5] intensity.

When the Stokes Raman-OTDR trace is used to normalize the AS trace [3], [6], we can obtain the following temperature-dependent ratio

$$\begin{aligned} R(z) &= \frac{P_{\mathrm{AS}}(z)}{P_S(z)} \\ &= C_R(z)\exp\left\{-\int_0^z \left[\alpha_{\mathrm{AS}}(\xi)-\alpha_S(\xi)\right]d\xi\right\} \\ &\quad \times \exp\left[\frac{-h\Delta\nu}{k_B T(z)}\right] \end{aligned} \tag{1}$$

where $\Delta\nu$ is the frequency separation between anti-Stokes and pump signal, $h$ is the Planck constant, $k_B$ is the Boltzmann constant, $T\,(z)$ is the local fiber temperature, $\alpha_{\mathrm{AS}}$ and $\alpha_S$ are the attenuation coefficient at the anti-Stokes and Stokes wavelengths, and $C_R\,(z)$ is a constant that takes into account the differences in the Raman capture factor and the response of the receiver for the different wavelengths. Note that the ratio $R\,(z)$ depends on the differential WDL of the fiber. If this factor is properly characterized as a function of the distance, it can be corrected from (1).

Unfortunately, the WDL are not constant in time, and might change depending on external environmental conditions [6]–[8]. Hence, the ratio AS/S (or AS/Rayleigh) is expected to change during the sensor lifetime due to the ageing process or external harsh environmental conditions, leading then to significant errors in the temperature estimation [6], [13]. Such errors actually consist in the gradual deviation of the temperature trace with respect to the real value, effect that increases with the distance and turns to be a critical factor at long sensing distances. As a consequence, the single-ended scheme described by (1) turns out to be inappropriate for many applications since it requires a continuous calibration, which is not possible in many cases [6].

### *B. Double-Ended RDTS Systems Based on Anti-Stokes Raman Component Only*

In order to correct the above-mentioned problem, measurements can be performed in a double-ended configuration [6]. In such a scheme, pump pulses are alternatively sent into the sensing fiber from both fiber ends, so that the AS signal and either the Stokes or the Rayleigh component can be measured in both forward and backward directions. Then, the geometric mean is taken between traces acquired in the two opposite directions.

Even though the RDTS system requires access to both fiber-ends, this configuration has been demonstrated to provide a simple and effective solution to compensate differential attenuation issues [6]. However, the standard loop configuration alone does not provide a complete compensation of the differential WDL that can potentially change with time [14], [15]. Although the use of traces in forward and backward directions compensates for the effects of WDL on the temperature profile (i.e., possible distortions in the trace), differential losses induce a significant variation in the temperature sensitivity and an offset with respect to the real temperature [14]. To correct such effects, an internal calibration fiber spool at a known temperature value is typically used, providing a simple and effective method to auto-compensate possible temperature errors [6], [14].

In order to overcome the problems generated by WDL, different auto-compensation methods have been recently proposed for short-to-medium sensing distances using for instance two optical sources at different wavelengths [15] or using only the anti-Stokes component reflected from a mirror [9]. In the case of long sensing ranges, a technique based on the use of anti-Stokes traces only in double-ended (loop) configuration has been proposed to reduce the impact of WDL and to simplify the system using a single receiver scheme [10], [11]. Although a successful experimental validation of the method has been presented in [10], [11], the robustness of the sensor under variations of the fiber losses (e.g., fiber attenuation, local losses or WDL) has not been investigated so far.

In the following sections of this paper we theoretically and experimentally study the impact of time- and wavelength-dependent losses in RTDS systems based on Raman anti-Stokes traces only. We also analyze the robustness and sensing performance of the system under different loss conditions for medium-to-long sensing distances (>10 km range).

Assuming that $z = 0$ corresponds to the fiber input of an AS-only RDTS when the forward direction is measured, the

anti-Stokes power obtained in both forward ($P_{\mathrm{AS\_For}}(z)$) and backward ($P_{\mathrm{AS\_Back}}(z)$) directions can be expressed as [10]

$$P_{\mathrm{AS\_For}}(z) = C_{\mathrm{AS\_For}}(z)N_{\Omega} \times \exp\left\{-\int_0^z [\alpha_{\mathrm{AS}}(\xi)+\alpha_P(\xi)]\,d\xi\right\} \quad (2)$$

$$P_{\mathrm{AS\_Back}}(z) = C_{\mathrm{AS\_Back}}(z)N_{\Omega} \times \exp\left\{-\int_z^L [\alpha_{\mathrm{AS}}(\xi)+\alpha_P(\xi)]\,d\xi\right\} \quad (3)$$

where $C_{\mathrm{AS\_For}}(z)$ and $C_{\mathrm{AS\_Back}}(z)$ are constants that depend on the Raman capture factor at the anti-Stokes wavelength, $L$ is the fiber length, and $N_{\Omega}$ is the Bose-Einstein thermal population factor, given by [12]

$$N_{\Omega} = \left[\exp\left(\frac{h\Delta\nu}{k_B T(z)}\right) - 1\right]^{-1}. \quad (4)$$

The AS trace in loop configuration is calculated as the geometric mean of the AS traces measured in forward and backward directions, as follows:

$$\begin{aligned} P_{\mathrm{AS\_Loop}}(z) &= \sqrt{P_{\mathrm{AS\_For}}(z)\cdot P_{\mathrm{AS\_Back}}(z)} \\ &= C_{\mathrm{AS\_Loop}}(z)\left\{\exp\left[\frac{h\Delta\nu}{k_B T(z)}\right]-1\right\}^{-1} \\ &\quad\times \exp\left\{-\frac{1}{2}\int_0^L [\alpha_{\mathrm{AS}}(\xi)+\alpha_P(\xi)]\;d\xi\right\} \end{aligned} \quad (5)$$

where $C_{\mathrm{AS\_Loop}}(z) = \sqrt{C_{\mathrm{AS\_For}}(z)\cdot C_{\mathrm{AS\_Back}}(z)}$.

In practice, it is difficult to estimate the absolute fiber temperature using (5), mainly because of possible inaccuracies when determining the coefficient $C_{\mathrm{AS\_Loop}}(z)$, value that can differ from fiber to fiber. Therefore, the sensor has to be calibrated to correct for the different Raman cross-sections when using different fiber spools. This can be done by normalizing the AS trace in loop configuration by another AS trace at a known reference temperature $T_{\mathrm{ref}}(z)$, similarly to what is typically done in standard AS/S double-ended RDTS systems. Thus, assuming no changes in the fiber losses, from (5) we obtain

$$\frac{P_{\mathrm{AS\_Loop}}(z,T)}{P_{\mathrm{AS\_Loop\_ref}}(z,T_{\mathrm{ref}})} = \left\{\exp\left[\frac{h\Delta\nu}{k_B T(z)}\right]-1\right\}^{-1} \times\left\{\exp\left[\frac{h\Delta\nu}{k_B T_{\mathrm{ref}}(z)}\right]-1\right\} \quad (6)$$

and therefore, we can calculate the temperature as [9], [10]:

$$T(z) = \left\{\frac{k_B}{h\Delta\nu}\ln\left[\frac{P_{\mathrm{AS\_Loop\_ref}}(z,T_{\mathrm{ref}})}{P_{\mathrm{AS\_Loop}}(z,T)} \times\left[\exp\left(\frac{h\Delta\nu}{k_B T_{\mathrm{ref}}}\right)-1\right]+1\right]\right\}^{-1}. \quad (7)$$

If we look at (5), we can notice that the use of the AS traces only in loop configuration allows for the compensation of local and distributed losses along the sensing fiber, in a similar way as the standard AS/S loop configuration does [6]. This means that there is no $z$ -dependent factor that could tilt or distort the temperature profile as a function of the distance, as in the case of single-ended schemes (described by (1)). Actually, it is important to notice that the exponential factor in (5) accounts for the total losses of the whole fiber at the pump and AS wavelengths, and not only for the differential losses. As a consequence, changes in the fiber attenuation (with respect to the initial calibration) are expected to introduce a $z$-independent constant multiplicative factor that modifies the final temperature profile. Thus, in case the fiber losses change with respect to the initial calibration, we have

$$\frac{P_{\mathrm{AS\_Loop}}(z,T)}{P_{\mathrm{AS\_Loop\_ref}}(z,T_{\mathrm{ref}})} = \left\{\exp\left[\frac{h\Delta\nu}{k_B T(z)}\right]-1\right\}^{-1} \times\left\{\exp\left[\frac{h\Delta\nu}{k_B T_{\mathrm{\_ref}}(z)}\right]-1\right\}\Delta l^{1/2} \quad (8)$$

where $\Delta l$ is the fiber loss variation with respect to the calibration, defined as

$$\Delta l = \exp\left\{-\int_0^L \Delta\alpha(\xi)\,d\xi\right\} \quad (9)$$

with

$$\begin{aligned} \Delta\alpha(\xi) &= [\alpha_{\mathrm{AS}}(\xi)-\alpha_{\mathrm{AS\_ref}}(\xi)]+[\alpha_P(\xi)-\alpha_{\mathrm{P\_ref}}(\xi)] \\ &= [\alpha_{\mathrm{AS}}(\xi)+\alpha_P(\xi)]-[\alpha_{\mathrm{AS\_ref}}(\xi)+\alpha_{\mathrm{P\_ref}}(\xi)]. \end{aligned} \quad (10)$$

Hence, the final temperature can be obtained as

$$T(z) = \left\{\frac{k_B}{h\Delta\nu}\ln\left[\frac{P_{\mathrm{AS\_Loop\_ref}}(z,T_{\mathrm{ref}})\Delta l^{1/2}}{P_{\mathrm{AS\_Loop}}(z,T)} \times\left[\exp\left(\frac{h\Delta\nu}{k_B T_{\mathrm{ref}}}\right)-1\right]+1\right]\right\}^{-1}. \quad (11)$$

In (11) we can notice that $\Delta l$ is a $z$-independent constant that uniformly impacts on the whole temperature trace, and therefore, the temperature trace is not tilted, as in single-ended schemes, but shifted by a constant value. In fact, the factor $\Delta l$ not only changes the offset of the measurements but also the temperature sensitivity of the whole system, resulting in a relevant issue to be addressed. In general terms, the factor $\Delta l$ accounts for any kind of variation in the total fiber attenuation, including distributed and local losses, which are expected to produce analogous effects in the final temperature profile. The impact of $\Delta l$ is actually similar to what WDL produce in RDTS systems based on conventional loop scheme, and therefore, the simple correction method employed in AS/S loop configuration [6] can also be used in the AS-only approach. In particular, the loss variation factor $\Delta l$ can be corrected in 'real-time' from (11) along the whole sensing fiber using the known reference temperature $T_{\mathrm{ref}}(z)$ used for calibration and the 'real-time' temperature $T(z)$ of a particular fiber spool (as for instance, in a fiber spool placed inside the RDTS, whose temperature can be measured with an additional electronic sensor). Thus, the calculated factor $\Delta l$ can then be used for temperature correction along the whole sensing fiber.

### C. Performance Improvement in RDTS Systems Based on AS-Only Scheme

Based on the signal and noise levels on both forward and backward AS traces ($S_{\mathrm{For}}, S_{\mathrm{Back}}, n_{\mathrm{For}}, n_{\mathrm{Back}}$), and under the assumption of uncorrelated, zero mean noise, the final SNR resulting from the AS-only loop scheme can be obtained as

$$\mathrm{SNR}_{\mathrm{AS\_Loop}}(z) = \frac{2S_{\mathrm{For}}(z)S_{\mathrm{Back}}(z)}{\sqrt{S^2_{\mathrm{For}}(z)n^2_{\mathrm{Back}}(z) + S^2_{\mathrm{Back}}(z)n^2_{\mathrm{For}}(z)}} = \frac{2}{\sqrt{\left(\frac{1}{\mathrm{SNR}_{\mathrm{For}}(z)}\right)^2 + \left(\frac{1}{\mathrm{SNR}_{\mathrm{Back}}(z)}\right)^2}} \quad (12)$$

where $\mathrm{SNR}_{\mathrm{For}}(z)$ and $\mathrm{SNR}_{\mathrm{Back}}(z)$ are the signal-to-noise ratio of the forward and backward AS traces.

In principle, (12) can also be applied to calculate the SNR of the resulting trace in standard AS/S loop configuration. In such a case, $S_{\mathrm{For}}$ and $S_{\mathrm{Back}}$ represent the AS/S ratio in forward and backward directions, while $n_{\mathrm{For}}$ and $n_{\mathrm{Back}}$ are the noise levels resulting from the respective ratio. Equation (12) then allows us to evaluate the sensing performance improvement provided by the AS-only scheme in comparison to the standard AS/S loop scheme. Actually, while in the case of AS-only scheme, $\mathrm{SNR}_{\mathrm{For}}(z)$ and $\mathrm{SNR}_{\mathrm{Back}}(z)$ represent the signal-to-noise ratio of the forward and backward AS traces, in the case of standard loop configuration, $\mathrm{SNR}_{\mathrm{For}}(z)$ and $\mathrm{SNR}_{\mathrm{Back}}(z)$ represent the signal-to-noise ratio of the AS/S ratios ($\mathrm{SNR}_{\mathrm{AS}/S}(z)$) in both directions, which can be evaluated as

$$\mathrm{SNR}_{\mathrm{AS}/S}(z) = \frac{1}{\sqrt{\left(\frac{1}{\mathrm{SNR}_{\mathrm{AS}}(z)}\right)^2 + \left(\frac{1}{\mathrm{SNR}_{S}(z)}\right)^2}} \quad (13)$$

where $\mathrm{SNR}_{\mathrm{AS}}(z)$ and $\mathrm{SNR}_{S}(z)$ are the signal-to-noise ratio of the respective anti-Stokes and Stokes traces.

Comparing (12) resulting from an AS-only loop scheme with (12) resulting from a standard loop (and using (13) for $\mathrm{SNR}_{\mathrm{For}}$ and $\mathrm{SNR}_{\mathrm{Back}}$) we can see that RDTS systems based on the AS-only scheme always have an improved SNR in comparison to standard AS/S loop configuration. In particular, when both Stokes and anti-Stokes traces have similar SNR, an improvement of 1.5 dB is expected, leading to a temperature resolution enhancement of a factor $\sqrt{2}$ with respect to the conventional technique.

## III. Results for Long-Distance RDTS Systems Using Anti-Stokes Raman Component Only

### A. Experimental Setup

In order to study the sensing capabilities of the proposed technique, the experimental setup shown in Fig. 1 has been used. A pulsed rare-earth doped fiber laser operating at 1550 nm (maximum peak power of 50 W at the minimum repetition rate of 2.5 kHz) and with 10 ns pulsewidth has been used to test the fiber with a meter-scale spatial resolution. The laser is non-polarized, thus avoiding any possible effect due to polarization-dependent losses on the temperature trace. By using a variable optical attenuator (VOA1), the peak power of the laser has been reduced to avoid nonlinear effects along the sensing fiber (15 W pulse peak power at the fiber input). A 3-port band combiner (filter full-width half maximum for the AS port equal to ∼30 nm) is used to launch pulses into the sensing fiber (passing through a $1 \times 2$ optical switch with an insertion loss of ∼0.5 dB per port) and to extract the backscattered AS Raman component centered at 1450 nm (pump to AS peak spectral separation equal to ∼13.2 THz), which is then measured by a single high-sensitivity receiver (details are given below). Both fiber ends have been connected to the sensor in loop configuration through the $1 \times 2$ optical switch, allowing pulses to be alternately sent in both forward and backward directions. A calibration unit, composed of an internal fiber spool and an electrical temperature sensor, is then used for temperature offset and sensitivity correction, as described in Section II-B.

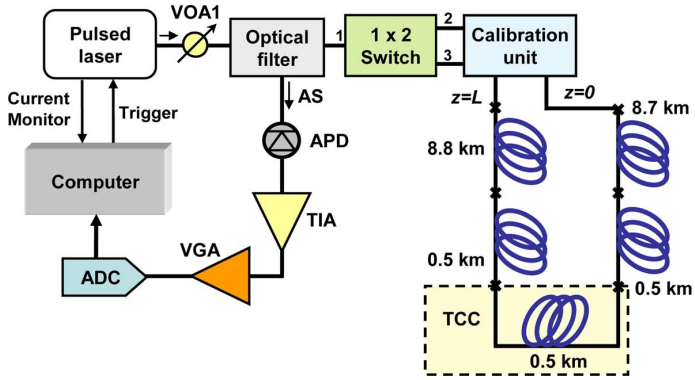


Fig. 1. Experimental setup of a long-range AS-only RDTS in loop scheme.

The sensing fiber is composed of five spools of graded-index 50/125 multimode fiber (all from same manufacturer but different production batches), allowing for a total sensing distance of 19 km. The middle fiber spool (500 m-long, at ∼9.3 km distance) has been placed inside a temperature-controlled chamber (TCC), whose temperature was changed during the experiment. The receiver is composed of a low-noise avalanche photodiode (APD), a trans-impedance amplifier (TIA) with 100 MHz bandwidth, a variable gain amplification stage (VGA) and a 14-bit analog-to-digital converter (ADC) with a sampling rate of 200 MS/s.

### B. Distributed Temperature Measurements

Anti-Stokes traces were continuously measured in both forward and backward directions with a total measurement time of ∼40 s (allowing for 100 k time-averaged traces). Fig. 2(a) shows the normalized AS traces in both directions at around 9.5 km distance, where 500 m of fiber have been placed inside a TCC. While the TCC temperature has been set to different values (−10°C, 10°C, 26.5°C and 50°C), the rest of the sensing fiber is kept at 26.5°C (room temperature). The temperature sensitivity of the implemented AS-only RDTS has been experimentally measured, resulting in 0.65%/°C, which is very close to the theoretical sensitivity expected for the AS component (∼0.8%/°C) [2].

The corresponding geometric mean of the AS traces in forward and backward directions is then calculated and reported in Fig. 2(b). We can see in the figure that the implemented scheme inherently cancels out fiber loss effects, as expected from the

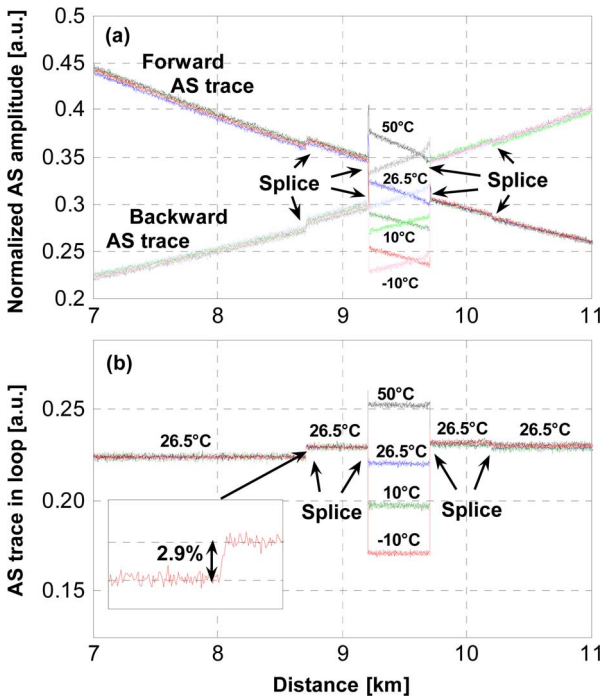


Fig. 2. (a) Normalized single-ended AS traces in forward and backward directions around the middle sensing fiber section, for different TCC temperature (b) Corresponding normalized AS traces in loop configuration.

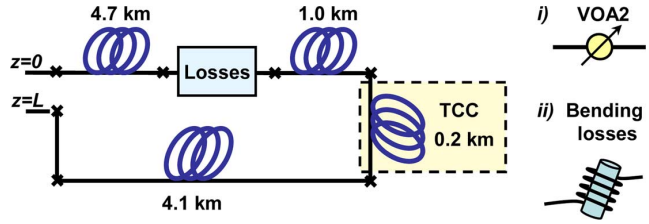


Fig. 3. Experimental fiber setup used to study the impact of *i*) local losses and *ii*) wavelength-dependent bending losses.

theory presented in Section II. However, it is worth noticing that, as described by (5), the intensity of the AS traces changes not only with temperature, but also depends on the Raman cross section of the different fiber spools used in the experiment. Actually, the inset in Fig. 2(b) indicates a variation of 2.9% in the spontaneous AS Raman intensity trace, between the first and second fiber spools (both at room temperature), due to differences in the Raman cross section of the fibers. This effect might potentially introduce errors in the temperature estimation, since the AS intensity variations (among different fiber spools) can be misinterpreted as temperature changes. Thus, for instance, a variation of 2.9% in the AS intensity could induce an accuracy error of $\sim$4.5°C in the estimated temperature profile. In order to account for this issue, and hence to avoid potential errors in the temperature estimation, a reference trace at a known temperature has been employed for the initial calibration, as described in Section II. In particular, the trace at room temperature (26.5°C) has been used to correct for this effect. Then, the final temperature profile can be estimated using (7) (in this case no loss variations have been introduced, and hence similar traces are expected from both (7) and (11)). As previously reported in [10], [11], results point out that the use of AS traces only in loop configuration provides similar characteristics as conventional RDTS systems, cancelling out local losses (such as splices) and fiber attenuation effects.

On the other hand, it is important to mention that this type of implementation also simplifies the data processing, since the use of only AS traces does not require the correction of the differential group-velocity between Stokes and anti-Stokes wavelengths, as needed in the standard AS/S loop scheme.

Note that the use of only AS traces makes the system sensitive to laser power variations, which can introduce distortions in the measured temperature profile. In order to compensate such possible fluctuations, we have studied two different techniques: *i*) the use of a built-in laser current monitor for AS trace normalization and *ii*) the use of a calibration unit containing a fiber spool at a well-known temperature (which is measured in 'real-time' with an electronic sensor). Experimental results have demonstrated that both techniques provide similar performance in terms of laser power variation compensation, leading in both cases to similar temperature profiles as the ones previously reported in [10], [11]. However, the use of the second method (i.e., the calibration unit) can be more practical since it allows us to overcome also the impact of externally-induced local losses (e.g., bending losses) as well as variations in the fiber attenuation (e.g., due to ageing process), as described in Section II-B, allowing one to provide reliable distributed temperature measurements. Therefore, the use of only the calibration unit is expected to be enough to provide reliable distributed temperature measurements, not requiring the use of a current monitor, as previously described. In Section IV, a detailed analysis is reported on the use of the internal fiber-spool correction method and the robustness of AS-only RDTS systems affected by local and wavelength-dependent losses.

## IV. Experimental Study on the Impact of Local and Wavelenght-Dependent Losses

### A. Experimental Setup

The experimental fiber configuration shown in Fig. 3 has been used to analyze the impact of local losses and WDL on the implemented AS-only RDTS system. In this case, we have employed the same experimental setup shown in Fig. 1; but the total fiber length has been decreased down to 10 km, allowing us to apply several dB of local losses and to perform a more reliable analysis of the traces with acceptable SNR values.

In order to evaluate the impact of local losses, we have followed two approaches. In the first approach (local losses), we have placed a variable optical attenuator (VOA2) at a 4.7 km distance (considered from the output port 2 of the optical switch) in order to introduce local losses. In the second approach (WDL), another set of measurements has been carried out replacing the VOA2 by 10 m of fiber where we have induced different wavelength-dependent bending losses (see setup *i*) and *ii*) in Fig. 3). One section of the sensing fiber ($\sim$200 m), at $\sim$5.7 km distance, has been placed inside the TCC, allowing for an accurate evaluation of the impact of the added losses on the sensing performance.

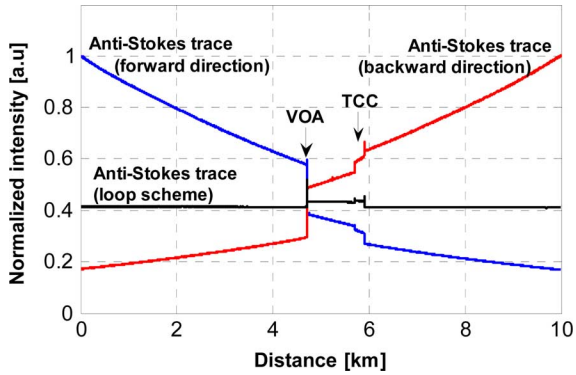


Fig. 4. Single-ended and double-ended AS traces used for RDTS calibration.

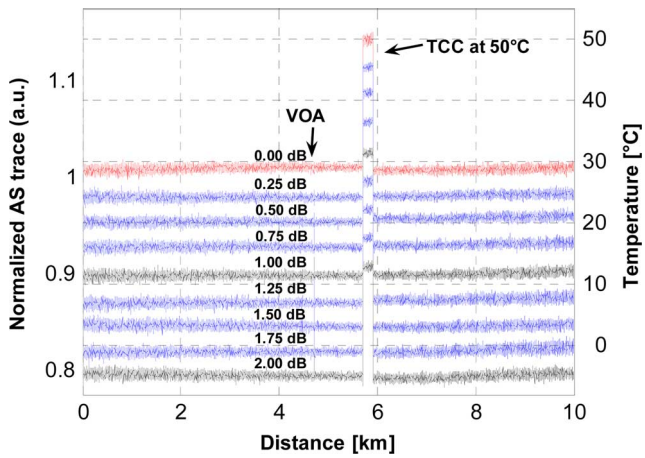


Fig. 5. Normalized AS traces (left-side axis) and consequent temperature profile (right-side axis) versus distance, when applying different local attenuations (up to 2 dB two-way losses).

### B. Impact and Compensation of Local Losses

To experimentally analyze the effects induced by local losses along the sensing fiber, the attenuation of the VOA2 has been changed from 0 dB up to 2 dB (in addition to the 1.7 dB two-way insertion loss affecting the AS trace) using steps of 0.25 dB. Anti-Stokes traces in loop scheme have been obtained through the geometric mean (as shown in Fig. 4) and then normalized with respect to the initial calibration trace at room temperature (VOA2 = 0 dB attenuation). With the initial calibration procedure, as in standard AS/S RDTS, we cancel out the effects of the Raman cross section of the different fiber spools as well as of the insertion loss of the VOA2.

Fig. 5 illustrates the impact of the added local attenuation over the normalized AS trace (see left-side vertical axis). We can observe that even though the geometric mean in the loop scheme compensates for possible distortions in the final AS trace, the multiplicative factor $\Delta l$ reduces the amplitude of the trace in loop when the attenuation is increased, as described by (8). Note that, the spatial resolution of the RDTS does not allow for the precise acquisition of the fast transient behavior generated by the VOA2, leading to a small peak in the traces at the position of the attenuator. This issue is partially compensated by the calibration trace, but is more evident for high local attenuation values. Fig. 5 also shows the temperature profile that the sensor would measure (as a function of the additional losses)

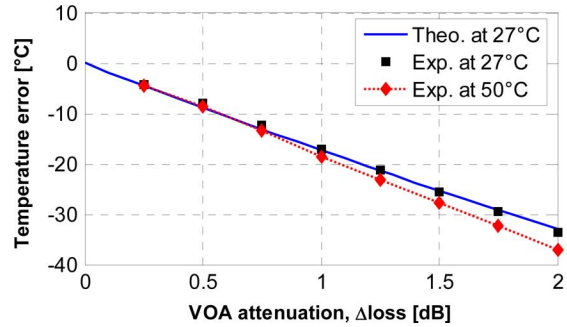


Fig. 6. Temperature error when no correction method is used.

if we did not compensate for this effect (see right-side vertical axis). We can observe that when no additional losses are introduced, the sensor is able to give a reliable measurement of the temperature (the room temperature was 27°C, and the TCC was set to 50°C). However, an increment in the local losses modifies the sensitivity and offset of the measured temperature profile, as described by (11). This effect is similar to the one produced by variations in the distributed fiber attenuation (as for instance due to ageing process), and also similar to what could result from WDL on RDTS systems based on the standard AS/S loop configuration. The impact of loss variations, as expected from theory and consistently with (11), is a constant multiplicative factor which is independent of the fiber location and depends on the total additional losses, as described by (9).

In Fig. 6 we compare the experimental and theoretical temperature deviation introduced by the additional fiber losses. The square points in Fig. 6 represent the experimental temperature error at room temperature as a function of the induced losses. We can observe that the experimental results agree with the expected theoretical errors, which are calculated from (11) and represented in the figure by the continuous line. Additionally, we have also investigated the temperature error induced in the fiber which is placed inside the TCC (at 50°C); we can observe in Fig. 6 that the error increases accordingly with the induced local losses. This behavior demonstrates that the error induced in the temperature is actually due to a multiplicative factor and not due to a simple temperature offset. In fact, this issue is visible also from Fig. 5, showing that the temperature gap of the fiber inside the TCC (at 50°C) is correctly measured as 23°C higher than the room temperature (27°C) when no attenuation is induced; but, this difference is erroneously reduced down to 17°C when the additional losses are 2 dB.

As previously mentioned, the temperature correction in the implemented sensor can be simply carried out by using a fiber spool inside the RDTS at a well known measured temperature. Fig. 7(a)–(d) actually shows the corrected temperature profiles that are measured with additional induced losses of 0 dB (a), 1 dB (b), 1.5 dB (c) and 2 dB (d). We can observe that the temperature profiles in Fig. 7 are properly corrected (in terms of offset and sensitivity) for all different applied local losses. The most critical case that we have analyzed in terms of potential temperature error is when the attenuation of the VOA2 was set to 2 dB. In this case we changed the temperature of the TCC between −10°C and 50°C; these temperature traces are shown in Fig. 8. As we can see in this figure, the use of the calibration

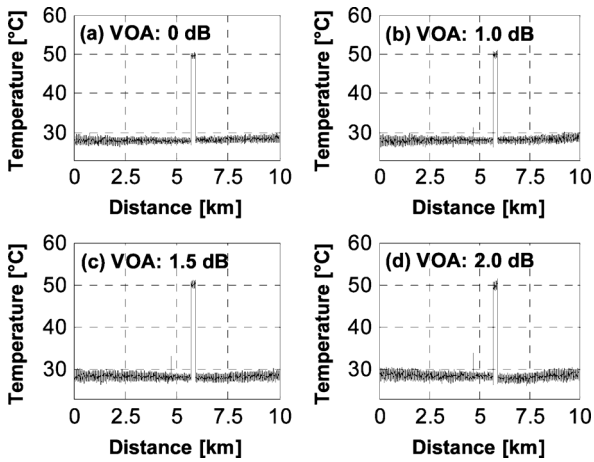


Fig. 7. Temperature profile versus distance obtained after correction, when applying different local losses.

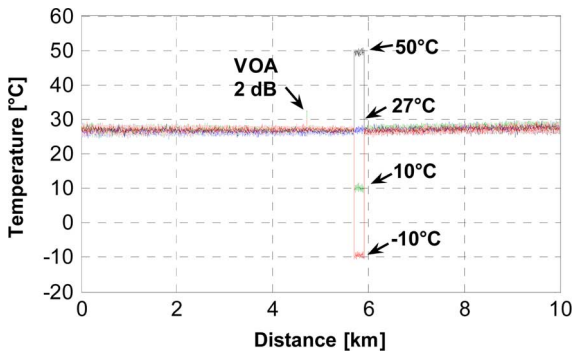


Fig. 8. Distributed temperature, obtained when applying 2 dB local losses, for different TCC temperatures.

unit allows for a proper correction of the temperature profile for all the cases, leading to reliable measurements with big temperature excursions.

### C. AS-Only RDTS Performance Under WDL Variations

In order to study the robustness of the AS-only RDTS system when differential WDL change along the sensing fiber, we replaced the VOA2 with 10 m of fiber (see Fig. 3), where we have induced different WDL through macroscopic bendings. By coiling the fiber around a cylinder of ∼1.5 cm diameter, and adjusting the number of turns, we induced several differential WDL values (such as 0.25 dB, 0.35 dB, 0.45 dB, and 0.55 dB WDL within the 1450–1650 nm range, which is mostly relevant for a sensible comparison with standard AS/S loop schemes).

Fig. 9 shows the temperature profile measured by the system in the four measurement scenarios, when the TCC has been set to 0°C. We can see that the AS-only RDTS is able to properly measure the temperature profile for all different WDL conditions. This is thanks to the calibration unit, with the internal fiber spool, which allows for the real-time correction of the temperature profile. As previously explained, even though we induced local WDL in our experiment, a similar behavior of the sensor is expected with equivalent distributed differential WDL, as for instance, resulting from fiber ageing process.

On the other hand, it is evident from Fig. 9(d) that the temperature resolution of the sensor was reduced significantly when the

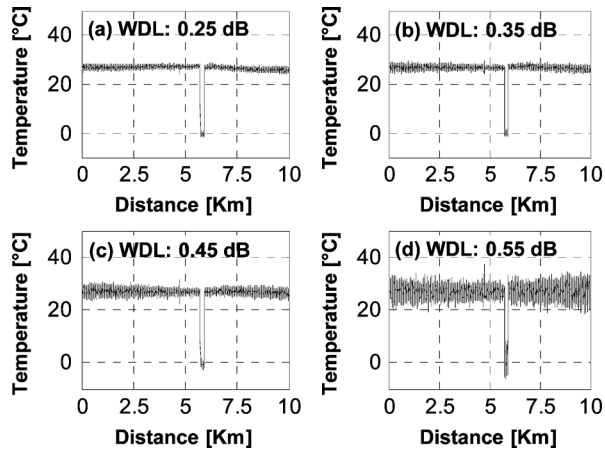


Fig. 9. Temperature profile as a function of the distance when applying different wavelength-dependent bending losses.

differential WDL reached 0.55 dB. However, this is due to the fact that forcing bending losses also increases the absolute local attenuation of the AS trace, which in that case was drastically increased up to more than 12 dB (two-way bending losses). Although the temperature resolution is worsened due to the much lower SNR in such a case, it is interesting to notice in Fig. 9(d) that the AS-only RDTS is still able to properly measure the distributed temperature profile.

## V. Performance Improvement in RDTS Systems Based on AS-Only Scheme

In order to analyze the sensing performance enhancement provided by the AS-only scheme, we compared the SNR of the system with the one obtained when using the conventional AS/S loop configuration. To carry out the measurements under similar experimental conditions, we have substituted the optical filter of the experimental setup in Fig. 1 with an optical filter which allows us to extract simultaneously the Stokes and anti-Stokes components. Then, the temperature and SNR profiles have been calculated using AS traces only or both Stokes and anti-Stokes traces.

Fig. 10 shows the SNR obtained with both AS-only and AS/S loop schemes when using 19 km of sensing fiber (similar to the setup shown in Fig. 1). While the continuous (noisy) lines were obtained by direct SNR calculation over both traces in loop configuration (AS-only and AS/S traces), the dashed lines were calculated from (12)–(13) using the SNR of the single-ended traces in forward and backward directions. We can see in Fig. 10 the good agreement between both theoretical and experimental results. As expected from the theory presented in Section II-C, the minimum SNR is obtained (in both cases) in proximity of the fiber ends. In particular, the fiber input $(z = 0)$ exhibits a lower SNR due to a small insertion-loss imbalance between the two output ports of the optical switch (see Fig. 1). When comparing the results of both loop schemes we can observe an SNR improvement of ∼1.3 dB in the case of AS-only. This is because the SNR in such a case only depends on the noise of the AS traces, and is not affected by the additional noise introduced by the Stokes intensity traces. This leads to an enhanced temperature resolution of ∼1.1°C (corresponding to ∼21.7 dB SNR) at

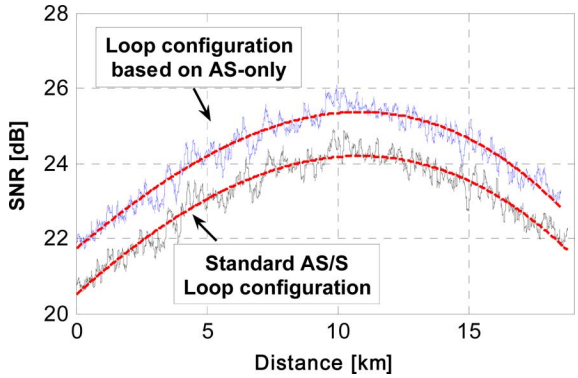


Fig. 10. SNR of the implemented long-range RDTS using AS-only scheme compared with standard AS/S loop configuration.

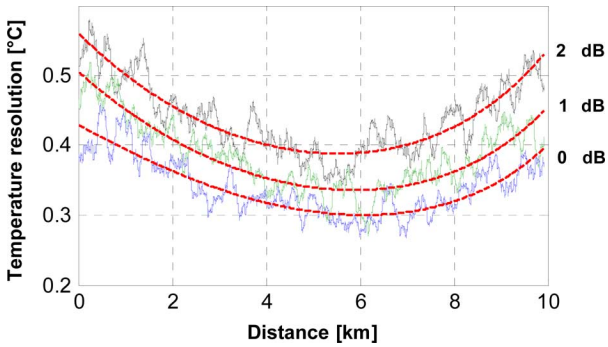


Fig. 11. Temperature resolution of the implemented 10 km-long RDTS using AS-only scheme compared when applying different local losses.

the fiber input when using the AS-only scheme, a value that is degraded to ∼1.5°C (∼20.4 dB SNR) when using the standard AS/S double-ended configuration.

When a shorter sensing fiber is used, the SNR of the AS-only loop configuration can be significantly improved. In particular, when we use a 10 km sensing fiber (as in the setup shown in Fig. 3), a temperature resolution of 0.43°C has been achieved, as shown in Fig. 11. This figure also illustrates the impact of the induced local losses (applied through the VOA2 as explained in Section IV.B) on the temperature resolution. We can observe that the added local losses $(\Delta l)$ impact on the whole SNR of the trace, and hence, on the whole temperature resolution (with no $z$ dependence), degrading it by a factor proportional to $\Delta l^{1/2}$. Thus, fiber losses of 1 dB and 2 dB degrade the temperature resolution from 0.43°C (at the fiber input) to 0.49°C and 0.56°C, respectively.

## VI. Conclusion

We have theoretically and experimentally analyzed the sensing capabilities of long-range RDTS systems based on the Raman anti-Stokes backscattered light only in a loop configuration. Experimental results demonstrate how this technique allows for the compensation of the impact of time- and wavelength-dependent loss variations along the sensing fiber, representing an interesting alternative to RDTS systems based on the traditional AS/S ratio. In addition, a theoretical description of the SNR improvement (and hence temperature resolution enhancement) in RDTS systems based on AS-only scheme has also been presented and experimentally validated.

## References

[1] B. Culshaw and A. Kersey, "Fiber-optic sensing: A historical perspective," *J. Lightwave Technol.*, vol. 26, no. 9, pp. 1064–1078, 2008.

[2] A. H. Hartog and A. P. Leach, "Distributed temperature sensing in solid-core fibres," *Electron. Lett.*, vol. 21, no. 23, pp. 1061–1062, Nov. 1985.

[3] J. P. Dakin and D. J. Pratt, "Distributed optical fibre Raman temperature sensor using a semiconductor light source and detector," *Electron. Lett.*, vol. 21, no. 13, pp. 569–570, 1985.

[4] K. Kikuchi, T. Naito, and T. Okoshi, "Measurement of Raman scattering in single-mode optical fiber by time-domain reflectometry," *IEEE J. Quantum Electron.*, vol. 24, no. 10, pp. 1973–1975, Oct. 1988.

[5] G. Bolognini, J. Park, M. A. Soto, N. Park, and F. Di Pasquale, "Analysis of distributed temperature sensing based on Raman scattering using OTDR coding and discrete Raman amplification," *Meas. Sci. Technol.*, vol. 18, pp. 3211–3218, 2007.

[6] A. F. Fernandez, P. Rodeghiero, B. Brichard, F. Berghmans, A. H. Hartog, P. Hughes, K. Williams, and A. P. Leach, "Radiation-tolerant Raman distributed temperature monitoring system for large nuclear infrastructures," *IEEE Trans. Nucl. Sci.*, vol. 52, no. 6, pp. 2689–2691, 2005.

[7] A. Kimura, E. Takada, K. Fujita, M. Nakazawa, H. Takahashi, and S. Ichige, "Application of a Raman distributed temperature sensor to the experimental fast reactor JOYO with correction techniques," *Meas. Sci. Technol.*, vol. 12, no. 7, pp. 966–973, Jul. 2001.

[8] M. Jaaskelainen, "Temperature monitoring of geothermal energy wells," in *Proc. of SPIE*, 2010, 7653, paper 765303.

[9] D. Hwang, D.-J. Yoon, I.-B. Kwon, D.-C. Seo, and Y. Chung, "Novel auto-correction method in a fiber-optic distributed-temperature sensor using reflected antistokes Raman scattering," *Opt. Exp.*, vol. 18, no. 10, pp. 9747–9754, 2010.

[10] M. A. Soto, A. Signorini, T. Nannipieri, S. Faralli, and G. Bolognini, "High-performance Raman-based distributed fiber-optic sensing under a loop scheme using antistokes light only," *IEEE Photon. Technol. Lett.*, vol. 23, no. 9, pp. 534–546, May 2011.

[11] M. A. Soto, A. Signorini, T. Nannipieri, S. Faralli, G. Bolognini, and F. Di Pasquale, "Distributed optical fiber temperature sensor using only antistokes Raman scattering light in a loop configuration," in *Proc. OFS21*, 2011, Paper 7753-384.

[12] M. N. Islam, "Raman Amplifiers for Telecommunications 1," in *Physical Principles*. New York: Springer-Verlag, 2004.

[13] P. R. Stoddart, P. J. Cadusch, J. B. Pearce, D. Vukovic, C. R. Nagarajah, and D. J. Booth, "Fibre optic distributed temperature sensor with an integrated background correction function," *Meas. Sci. Technol.*, vol. 16, no. 6, pp. 1299–1304, Jun. 2005.

[14] S. W. Tyler, J. S. Selker, M. B. Hausner, C. E. Hatch, T. Torgersen, C. E. Thodal, and S. G. Schladow, "Environmental temperature sensing using Raman spectra DTS fiber-optic methods," *Water Resour. Res.*, vol. 45, Jan. 2009, W00D23.

[15] K. Suh and C. Lee, "Auto-correction method for differential attenuation in a fiber-optic distributed-temperature sensor," *Opt. Lett.*, vol. 33, no. 16, pp. 1845–1847, Aug. 2008.

**Author biographies not included at authors' request due to space constraints.**